Pure white hybrid light-emitting device with color rendering index higher than 90

Gang Cheng,* Marco Mazzeo, Stefania D'Agostino, Fabio Della Sala, Sonia Carallo, and Giuseppe Gigli

National Nanotechnology Laboratory (NNL), CNR-INFM, Università del Salento, Via per Arnesano, Km 5, 73100 Lecce, Italy

**Corresponding author: gang.cheng@unile.it*

Received October 14, 2009; revised January 8, 2010; accepted January 12, 2010; posted January 14, 2010 (Doc. ID 118494); published February 19, 2010

The realization of white-light sources with a combination of high color rendering index (CRI), which is the average of the first eight rendering indices, and the deep-red color rendering R9 is an important challenge in the field of solid-state lighting. Herein, we report on a pure white hybrid light-emitting device combining a deep-blue emission from a polymer with blue, green, and red emissions from ternary CdSe/ZnS quantum dots. By carefully designing the device structure and tuning the ratio of QDs with different sizes, high CRI of 94 and R9 of 92 at 525 cd/m^2 were achieved. © 2010 Optical Society of America

OCIS codes: 160.4236, 230.3670, 250.5230, 260.3800.

In the field of lighting, an important figure of merit is represented by the color rendering index (CRI). This parameter is one of the key criteria for judging the quality of an artificial lighting system. The score for perfect color rendering is 100. CRI is typically given as R_a, which is the average of only the first eight rendering indices. The ninth rendering index R9 in particular is critical for deep-red rendering and is important in biomedical applications [1]. A combination of high CRI and the R9 is very interesting for commercial applications. Despite the rapid improvement of the efficiency of white organic light-emitting devices (LEDs) [2–5], devices with CRI > 90 have been rarely reported [6] because of the difficult realization of the fine tuning of color emission in organic compounds, which is very important for achieving high CRI. On the other hand, hybrid LEDs [7–13] based on organic materials and colloidal quantum dots (QDs) are theoretically advantageous for white-light generation due to the easy color modulation by simply tuning the size of the QDs [14]. To our knowledge, white hybrid LEDs with CRI > 90 have not been reported so far. We believe this is mainly because of the difficulty in the synthesis of deep-blue emitting QDs. In this Letter, we demonstrate that by combining deep-blue emission from poly[*N*,*N*′-bis(4-butylphenyl)-*N*,*N*′-bis(phenyl)benzidine] (poly-TPD) [15] with blue, green, and red emissions from ternary QDs, high CRI of 94 and R9 of 92 can be achieved in the hybrid LED with proper device structure and optimized ratio of blue, green, and red emitting QDs. The obtained result is in good agreement with theoretical calculation that predicts a maximum CRI of 96 for this hybrid system.

Core/shell CdSe/ZnS QDs (lake placid blue, catskill green, and maple red orange) were purchased from Evident Technologies Inc., poly(3,4-ethylenedioxythiophene):poly(styrene sulfonic acid) (PEDOT:PSS) from H. C. Starck GmbH, poly-TPD from American Dye Source Inc., 4,4′-*N*,*N*′-dicarbazole-biphenyl (CBP) and 2,2′,2″-(1,3,5-phenylene) tris (1-phenyl-1H-benzimidazole) (TPBI) from Sensient Imaging Technologies GmbH. As shown in the inset of Fig. 1(a), all devices studied in this work have a structure of ITO/PEDOT:PSS/poly-TPD (20 nm)/CBP:QDs(B,G,R) (40 nm)/ETL (40 nm)/LiF (0.5 nm)/Al (200 nm). TPBI is used as an electron-transporting layer (ETL) in TPBI devices, while replaced by Alq_3 in the control device (Alq_3 device). The fabrication and characterization details have been described in our previous papers [8,11,13].

Normalized electroluminescent (EL) spectrum of Alq_3 device at 10 V is shown as a red dashed line in

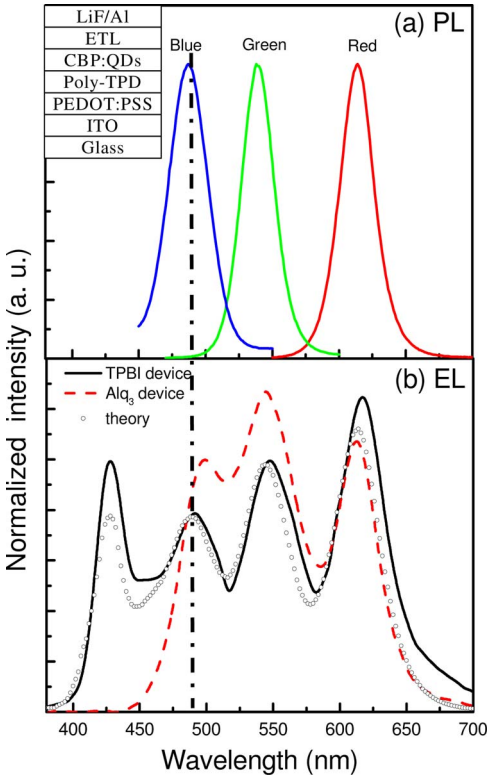

Fig. 1. (Color online) (a) PL spectra of blue, green, and red QDs in toluene. Inset, device structure studied in this work. (b) Normalized EL spectra of TPBI and Alq_3 devices. The dots represent the theoretical spectrum corresponding to the maximum possible CRI value. The dotted–dashed line indicates PL peak of blue QDs.

0146-9592/10/050616-3/$15.00

Table 1. Main Performances of Alq_3 Device

V (V)	L (cd/m^2)	EQE (%)	LE (cd/A)	PE (lm/W)	CRI
6	50	0.96	2.9	1.6	61
8	400	0.74	2.4	0.95	58
10	1800	0.53	1.7	0.52	55

Fig. 1(b). Three main emission peaks at 500, 550, and 620 nm are clearly observed. Comparing with Fig. 1(a), which shows the photoluminescent (PL) spectra (λ_{ex}=420 nm) of blue, green, and red QDs, we can conclude that the peaks at 550 and 620 nm come from the emissions of green and red QDs, respectively, while the peak at 500 nm redshifts about 10 nm relatively to PL of blue QDs, as indicated by the dotted–dashed line. The CRI of this device at high luminance is lower than 60 (see Table 1) due to the lack of deep-blue emission. By replacing Alq_3 by TPBI as ETL, the CRI is dramatically improved to 94 at 10 V (see Table 2). This improvement can be explained by EL spectrum of TPBI device shown as a black solid line in Fig. 1(b). Compared to Alq_3 device, an additional emission peak appears in the deep-blue region from poly-TPD [9], while the emission peak at 490 nm is identical to PL of blue QDs. By combining this deep-blue emission from poly-TPD with blue, green, and red emissions from ternary QDs, a broad EL emission covering almost the full visible spectrum is obtained, which consequently leads to a high CRI. To explain the different EL spectra of Alq_3 and TPBI devices, an EL diagram is proposed according to literatures [15–18] and shown in Fig. 2. In Alq_3 device, excitons formed in CBP layer tend to diffuse into Alq_3 layer, because its bandgap is narrower than that of poly-TPD or CBP. Although excitons are mainly trapped in QDs, some of them can eventually reach the Alq_3 layer, especially those formed at the Alq_3/CBP interface. In the Alq_3 layer, some of them transfer their energy to the low-energy QDs and enhance their intensity [11], while the others radiatively recombine in Alq_3 molecules. The overlap of emissions from Alq_3 (at 520 nm) and blue QDs causes the EL peak at 500 nm. In TPBI device, on the other hand, because of the wider bandgap of TPBI, excitons tend to diffuse to poly-TPD layer, who has the narrowest bandgap in this device. Therefore, similar to the processes in Alq_3 device, some excitons recombine in poly-TPD layer resulting in the deep-blue emission, while the others transfer energy to QDs. In hybrid LEDs, besides the direct charge injection, energy transfers occur from organic materials to QDs [11] and from high-energy to lower-energy QDs [19,20].

Table 2. Main Performances of TPBI Device

V (V)	L (cd/m^2)	EQE (%)	LE (cd/A)	PE (lm/W)	CRI
6	7.3	0.46	1.1	0.57	65
8	139	0.41	0.91	0.36	87
10	525	0.28	0.61	0.19	94

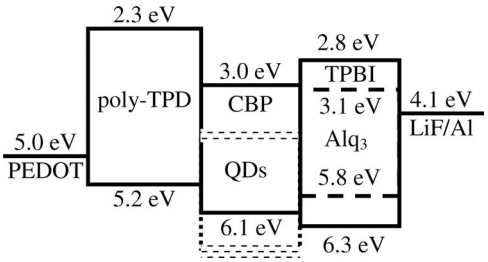

Fig. 2. (a) Proposed EL diagrams of Alq_3 and TPBI devices. Dashed lines indicate energy levels of Alq_3 and dotted lines indicate energy levels of QDs.

Since these energy transfers enhance the emissions of low-energy QDs, especially the red ones, high blue-QD concentration is necessary to achieve balanced white emission. We found that the optimal molar ratio for blue:green:red QDs is 38:5:2 in our case. As comparison, chromaticity properties of TPBI devices with various QD ratios at 10 V are also listed in Table 3.

In Fig. 1, we also show the spectrum corresponding to the maximum CRI value (96) achievable with this hybrid system. This spectrum was obtained by a three-dimensional optimization, considering all the possible EL spectra obtained by a linear combination of the individual EL spectra intensities (I) of poly-TPD and QDs. The final spectrum is given by

$$I(c_1,c_2,c_3;\lambda) = I_{poly-TPD}(\lambda) + c_1 I_{blue}(\lambda) + c_2 I_{green}(\lambda) + c_3 I_{red}(\lambda),$$

where the c_i represents the relative intensity of QDs respect to the poly-TPD. The CRI value for each $I(c_1,c_2,c_3;\lambda)$ spectrum has been computed by the emissive thin-film optics simulator (ETFOS) [21]. As shown Fig. 1, our experimental spectrum at 10V is in good agreement with the theoretical optimum one.

The characteristics of luminance (L) and luminous efficiency (LE) versus driving voltage (V) of both TPBI and Alq_3 devices are plotted in Fig. 3(a), while the curves of current density (J) and power efficiency (PE) versus V are described in Fig. 3(b). Since Alq_3 and poly-TPD are both involved in the emissions of the corresponding devices, as discussed previously, and the efficiency of former is higher than the latter, external quantum efficiency (EQE) of Alq_3 device is higher than that of TPBI device (see Tables 1 and 2), resulting in higher L and LE. Therefore, PE of Alq_3

Table 3. Chromaticity of TPBI Devices with Various QD Ratios

Molar ratio of QDs (blue:green:red)	CCT (K)	CIE coordinates (x,y)	CRI	R9
38:5:2	4719	0.35, 0.35	94	92
38:5:1	7401	0.28, 0.38	65	−55
38:5:4	2185	0.45, 0.33	75	77
38:2:2	6946	0.32, 0.27	62	3
38:10:2	4123	0.38, 0.44	75	19

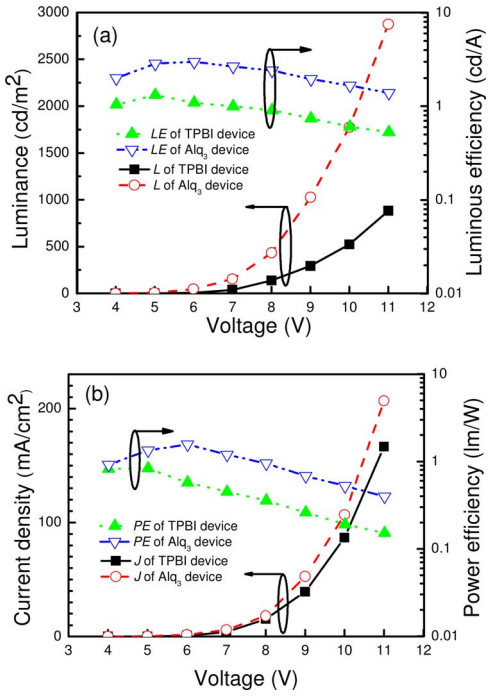

Fig. 3. (Color online) (a) L-LE-V characteristics of Alq_3 and TPBI devices. (b) J-PE-V characteristics of Alq_3 and TPBI devices.

device is also higher considering the similar J-V curves shown in Fig. 3(b). Furthermore, imbalanced charge injection to QDs and the resulting exciton recombination via Auger mechanism might be another reason for the lower efficiency of TPBI device [18]. The measured maximum CRI of 94 in TPBI device is much higher because of the absence of the deep-blue emission in Alq_3 device.

In summary, we demonstrated a greenish white hybrid LED with a maximum EQE of 0.96% and a maximum PE of 1.6 lm/W using ternary QDs doped CBP as an EML, Alq_3 as an ETL, and poly-TPD as an hole-transporting layer. When Alq_3 was replaced by TPBI, strong deep-blue emission from poly-TPD was observed due to the wide bandgap of TPBI. By combining this deep-blue emission with the emissions of ternary QDs, a pure white LED with Internationale De L'Eclairage (CIE) coordinates of (0.35, 0.35), CRI of 94, and R9 of 92 at 525 cd/m^2 was realized.

This work is partially funded by the ERC-Starting Grant FP7-Project "DEDOM," grant agreement no. 207441.

References

1. M. R. Krames, O. B. Shchekin, R. Mueller-Mach, G. O. Mueller, L. Zhou, G. Harbers, and M. G. Craford, J. Disp. Technol. **3**, 160 (2007).
2. G. Cheng, F. Li, Y. Duan, J. Feng, S. Y. Liu, S. Qiu, D. Lin, Y. G. Ma, and S. T. Lee, Appl. Phys. Lett. **82**, 4224 (2003).
3. G. Cheng, Y. F. Zhang, Y. Zhao, Y. Y. Lin, C. Y. Ruan, S. Y. Liu, T. Fei, Y. G. Ma, and Y. X. Cheng, Appl. Phys. Lett. **89**, 043504 (2006).
4. Y. Sun, N. C. Giebink, H. Kanno, B. Ma, M. E. Thompson, and S. R. Forrest, Nature **440**, 908 (2006).
5. S. Reineke, F. Lindner, G. Schwartz, N. Seidler, K. Walzer, B. Lüssem, and K. Leo, Nature **459**, 234 (2009).
6. Novaled AG, http://www.novaled.com/news/2007_11_05_pr.html.
7. M. Gao, B. Richter, and S. Kirstein, Adv. Mater. **9**, 802 (1997).
8. Y. Li, A. Rizzo, M. Mazzeo, L. Carbone, L. Manna, R. Cingolani, and G. Gigli, J. Appl. Phys. **97**, 113501 (2005).
9. Z. Tan, B. Hedrick, F. Zhang, T. Zhu, J. Xu, R. H. Henderson, J. Ruzyllo, and A. Y. Wang, IEEE Photon. Technol. Lett. **20**, 1998 (2008).
10. A. Rizzo, M. Mazzeo, M. Biasiucci, R. Cingolani, and G. Gigli, Small **4**, 2143 (2008).
11. Y. Li, A. Rizzo, R. Cingolani, and G. Gigli, Adv. Mater. **18**, 2545 (2006).
12. P. O. Anikeeva, J. E. Halpert, M. G. Bawendi, and V. Bulović, Nano Lett. **7**, 2196 (2007).
13. G. Cheng, M. Mazzeo, A. Rizzo, Y. Li, Y. Duan, and G. Gigli, Appl. Phys. Lett. **94**, 243506 (2009).
14. S. Nizamoglu, G. Zengin, and H. V. Demir, Appl. Phys. Lett. **92**, 031102 (2008).
15. Q. J. Sun, J. H. Hou, C. H. Yang, Y. F. Li, and Y. Yang, Appl. Phys. Lett. **89**, 153501 (2006).
16. T. Tsuzuki and S. Tokito, Adv. Mater. **19**, 276 (2007).
17. S. Coe-Sullivan, W.-K. Woo, J. S. Steckel, M. Bawendi, and V. Bulović, Org. Electron. **4**, 123 (2003).
18. P. O. Anikeeva, J. E. Halpert, M. G. Bawendi, and V. Bulović, Nano Lett. **9**, 2532 (2009).
19. C. R. Kagan, C. B. Murry, M. Nirmal, M. G. Bawendi, and V. Bulović, Phys. Rev. Lett. **76**, 1517 (1996).
20. S. A. Crooker, J. A. Hollingsworth, S. Tretiak, and V. I. Klimov, Phys. Rev. Lett. **89**, 186802 (2002).
21. Fluxim AG, Switzerland, http://www.fluxim.com.